

Variations in PM_{2.5}, TSP, BC, and trace gases (NO₂, SO₂, and O₃) between haze and non-haze episodes in winter over Xi'an, China

Qian Zhang^{a,b}, Zhenxing Shen^{a,b,*}, Junji Cao^b, Renjian Zhang^c, Leiming Zhang^d, R.-J. Huang^{b,e,f}, Chenjia Zheng^a, Linqing Wang^a, Suixin Liu^b, Hongmei Xu^a, Chunli Zheng^a, Pingping Liu^a

^a Department of Environmental Science and Engineering, Xi'an Jiaotong University, Xi'an 710049, China

^b Key Lab of Aerosol Chemistry & Physics, Institute of Earth Environment, Chinese Academy of Sciences, China

^c Key Laboratory of Regional Climate-Environment Research for Temperate East Asia, Institute of Atmospheric Physics, Chinese Academy of Sciences, Beijing 100029, China

^d Air Quality Research Division, Science and Technology Branch, Environment Canada, Toronto, Canada

^e Laboratory of Atmospheric Chemistry, Paul Scherrer Institute (PSI), 5232 Villigen, Switzerland

^f Centre for Climate and Air Pollution Studies, Ryan Institute, National University of Ireland Galway, University Road, Galway, Ireland

HIGHLIGHTS

- The diurnal cycle of BC and trace gases pattern showed remarkable difference between haze and non-haze days.
- SO₄²⁻/EC, NO₃⁻/EC, and NH₄⁺/EC were sharply increasing from non-haze period to haze days in comparison with OC/EC.
- Wintertime haze secondary organic carbon (SOC) accounts for nearly one third of OC level.

ARTICLE INFO

Article history:

Received 31 January 2015

Received in revised form

11 April 2015

Accepted 13 April 2015

Available online 15 April 2015

Keywords:

Aerosol formation

Inorganic aerosol

Organic aerosol

Secondary aerosol

Urban environment

ABSTRACT

To investigate chemical profiles and formation mechanisms of aerosol particles in winter haze events, daily PM_{2.5} and TSP, 5-min BC, and 15-min trace gases (SO₂, NO₂, and O₃) were measured continuously during Dec. 1–31, 2012 in Xi'an. Chemical analysis was also conducted for nine water-soluble inorganic ions (Na⁺, NH₄⁺, K⁺, Mg²⁺, Ca²⁺, F⁻, Cl⁻, NO₃⁻, and SO₄²⁻), organic carbon (OC), elemental carbon (EC), and eight carbon fractions (OC1, OC2, OC3, OC4, EC1, EC2, EC3, and OP) in both PM_{2.5} and TSP samples. Higher levels of TSP, PM_{2.5}, BC, SO₂, and NO₂, and lower levels of O₃ were observed during haze periods in comparison with non-haze days. The sum of the major secondary ionic species (NH₄⁺, NO₃⁻, and SO₄²⁻) in PM_{2.5} or TSP during haze periods was about 3 times of that during non-haze days. Ion balance calculations showed that PM_{2.5} samples were acidic during haze periods and were close to neutral during non-haze days. The mean carbon levels were 52.9 μg m⁻³ and 82.1 μg m⁻³ in PM_{2.5} and TSP, respectively, during haze events, which were ~1.5 times of those during non-haze days. The diurnal variations of BC during non-haze days showed a bimodal distribution with two peaks coincided with traffic rush hours. This was not the case during haze periods, which exhibited a relatively smooth pattern but with high concentration levels, providing evidence of particle accumulation. The ratios of SO₄²⁻/EC, NO₃⁻/EC, and NH₄⁺/EC sharply increased during haze periods, indicating the important pathway of secondary inorganic species formation through aqueous-phase transformation under high relative humidity condition. This study also highlights that wintertime secondary organic carbon (SOC) formation can be an important contributor to carbonaceous aerosol, especially during haze periods.

© 2015 Elsevier Ltd. All rights reserved.

* Corresponding author. Department of Environmental Science and Engineering, Xi'an Jiaotong University, Xi'an 710049, China.

E-mail address: zxshen@mail.xjtu.edu.cn (Z. Shen).

1. Introduction

Haze is a worldwide environmental issue and receives increasing attention due to its impact on visibility, air quality, radiative forcing, regional climate, and human health (Schichtel

et al., 2001; Chen et al., 2003; Yadav et al., 2003; Kang et al., 2004; Jung et al., 2009; Huang et al., 2014). Haze is defined as a condition in which the atmospheric visibility is less than 10 km by China Meteorological Agency (http://www.cma.gov.cn/zcfg/qxbz/bzzqyj/index_5.html). Previous studies have shown that haze is closely related to meteorological conditions and the levels of air pollutants including gaseous species (e.g. SO₂ and NO_x) and particulate matter (PM). For example, sharp increases of ~30% of SO₂, ~28% of NH₃, ~40% of PM_{2.5}, ~45% of PM₁₀ and ~60% of TSP have been observed during various pollution episodes in China (Oanh and Leelasakultam, 2011; Chang et al., 2011; Shen et al., 2009; Du et al., 2011).

The chemical characteristics and formation mechanisms of aerosol particles could be different between haze and non-haze events (Shen et al., 2009; Odmana et al., 2009; Wang et al., 2006; Chang et al., 2011; Oanh and Leelasakultam, 2011; Du et al., 2011; Huang et al., 2014). For example, Huang et al. (2014) reported that the winter severe haze pollution events were driven to a large extent by secondary aerosol (such as SO₄²⁻, NO₃⁻, NH₄⁺, and OC) formations, which contributed 30–77% of PM_{2.5} and 44–71% of organic aerosols. A more recent study by Tao et al. (2015) also showed that concentrations of SO₄²⁻, NO₃⁻ and NH₄⁺ increased much more than those of OC and EC during heavy-polluted periods compared to those during light-polluted or clean periods in a winter season in Beijing.

Xi'an, the capital city of Shaanxi province in Northeast China, is located in the Guanzhong Plain area with a topographic basin surrounded by Qinling Mountains to the south and the Loess Plateau to the north. Similar to many other mega cities in China, Xi'an is facing long-term air quality concerns with PM pollution being a major concern due to rapidly increased vehicle traffic and energy consumption during the past several decades (Shen et al., 2008, 2009, 2011; Cao et al., 2012). The annual precipitation amount (~600 mm) is relatively low and cannot alleviate pollution levels to meet the national air quality standard (Shen et al., 2012). Several earlier studies in this city only focused on aerosol properties without the knowledge of gaseous precursors (Cao et al., 2009; Yan et al., 2013; Cheng et al., 2013; Shen et al., 2014). In the present study, chemically resolved PM_{2.5} and TSP, black carbon, and gaseous pollutants (NO₂, SO₂, and O₃) were simultaneously determined to obtain a complete picture of pollution events and to investigate PM formation mechanisms during winter haze episodes in Xi'an, China.

2. Data sampling and chemical analysis

2.1. Data sampling

Integrated PM_{2.5} and TSP samples, online gaseous pollutants (NO₂, SO₂, and O₃), and BC were collected simultaneously from 1 Dec. to 31 Dec. 2012 on the roof of a 15 m high building located about 100 m north of the South Second Ring Road in the southeastern part of downtown Xi'an (Fig. 1). The north and east sides of the sampling site are residential areas and the campus of Xi'an Jiaotong University, and the south and west sides are major roads with heavy traffics.

24 h (9:00 a.m. to 9:00 a.m. the following days) PM_{2.5} and TSP samples were collected on quartz filters (47-mm diameter cellulose nitrate membranes) using a dual-channel low-volume sampler (Tokyo Dylec) operating at the flow rate of 5 L min⁻¹. A total of 62 aerosol samples were collected, equilibrated for 24 h at 20–23 °C in a chamber with a relative humidity between 35% and 45%, and weighed at least three times following the 24-h equilibration period. Three strong haze episodes were observed during Dec. 1–2, Dec. 9–16, and Dec. 24–28, respectively. Artifacts for ionic species (such as ammonium) and OC are expected during sampling,

however, are believed to be small because the study used the mini-vol sampler with 5 L min⁻¹ to collect aerosol samples. The measured ionic species and total carbon concentrations were also much higher than anticipated artifacts from the filters during this study. Thus, the samples were only corrected for blank filters to obtain the ionic species and OC concentrations.

BC measurements were conducted with the multi-angle absorption photometer (MAAP) (Thermo Scientific), which was based on the principle of aerosol light absorption and the corresponding atmospheric BC mass concentration at the wavelength of 637 nm (Sheridan et al., 2005). The MAAP-5012 can reduce the uncertainties of the measured aerosol absorption coefficient and was operated continuously at a stable airflow rate of 5 L min⁻¹ with a time resolution of 5 min (Petzold et al., 2002). In addition, the ambient O₃ (Model ML/EC9810, Ecotech Pty Ltd, Australia), NO₂ (Model ML/EC9841B Analyzer, Ecotech Pty Ltd, Australia), and SO₂ (Model ML/EC9850 Analyzer, Ecotech Pty Ltd, Australia) were continuously measured every 5-min during sampling periods. Zero checks were performed every day by automatically injecting charcoal-scrubbed air. Meteorological data, including temperature, relative humidity (RH), wind speed, and visibility were recorded by the Shanxi meteorological agency at a meteorological station about 10 km north of the sampling site.

2.2. PM chemical analysis

To analyze the cations and anions (Na⁺, NH₄⁺, K⁺, Mg²⁺, Ca²⁺, F⁻, Cl⁻, NO₃⁻, and SO₄²⁻), one fourth of each filter sample was put into a separate 20 mL vial containing 10 mL distilled-deionized water (a resistivity of 18.3 MΩ), placed in ultrasonic water bath for 60 min, and shaken by mechanical shaker for 1 h for complete extraction of the ionic compounds. The extracts were filtered 1–3 times with a 0.45 μm pore size microporous membrane, and then stored at 4 °C in a clean tube before analysis. The series of concentrations were analyzed by an ion chromatography (IC, Dionex 500, Dionex Corp, Sunnyvale, California, United States). The limits of detection were less than 0.05 mg L⁻¹ for analysis, one sample in each group of ten samples was selected to analyze twice for quality control purposes. Detail description of ions analysis can be found in Shen et al. (2007, 2008).

A 0.5 cm² punch of each sample was analyzed for EC and OC in this study following Interagency Monitoring of Protected Visual Environments (IMPROVE) thermal/optical reflectance protocol by using a DRI Model 2001 Thermal and Optical Carbon Analyzer (Atmoslytic Inc., Calabasas, CA, USA). Four OC fractions (OC1, OC2, OC3, and OC4 at 140 °C, 280 °C, 480 °C, and 580 °C, respectively, in a helium atmosphere), and three EC fractions (EC1, EC2, and EC3 at 580 °C, 740 °C, and 840 °C, respectively, in a 2% oxygen/98% helium atmosphere) were produced. During volatilization of organic carbon, part of organic carbon was converted pyrolytically to EC (this fraction of OC was named as OP) (Chow et al., 2004). Hence, OC is the sum of OC1, OC2, OC3, OC4, and OP, and EC is the sum of EC1, EC2, and EC3 and then minus OP. Additional quality assurance and quality control procedures have been described in detail in Cao et al. (2003).

3. Results and discussion

3.1. PM, BC, and trace gases levels during haze and non-haze days

Table 1 shows the average concentrations of several atmospheric pollutants (PM_{2.5}, TSP, BC, SO₂, NO₂, and O₃) and the meteorological conditions (visibility, temperature, relative humidity and wind speed) during both haze and non-haze periods. The daily averaged PM_{2.5} and TSP concentrations were significantly higher during haze

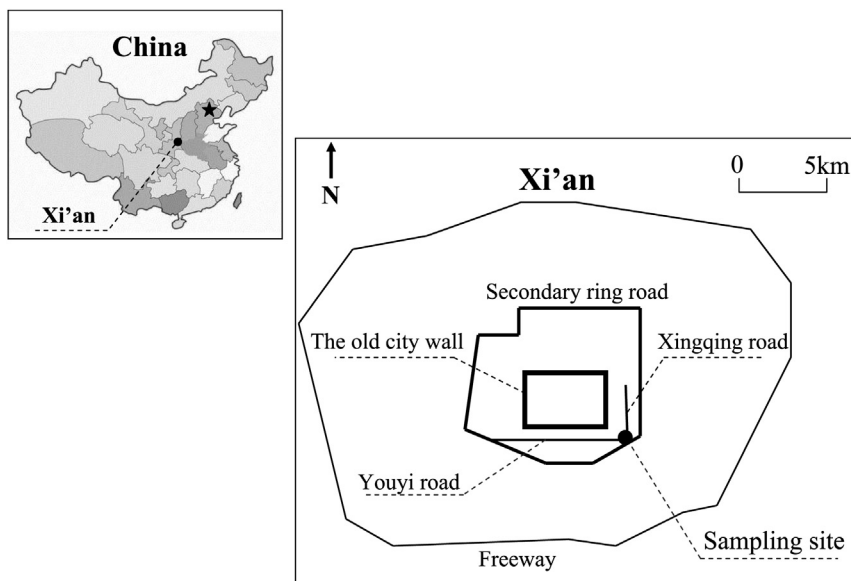


Fig. 1. Location of the sampling site.

Table 1
Average values of meteorological parameters and air pollutants in haze and non-haze days, together with the ratios of non-haze/haze for each component.

Species		PM _{2.5} ($\mu\text{g m}^{-3}$)	TSP ($\mu\text{g m}^{-3}$)	BC ($\mu\text{g m}^{-3}$)	SO ₂ ($\mu\text{g m}^{-3}$)	NO ₂ ($\mu\text{g m}^{-3}$)	O ₃ ($\mu\text{g m}^{-3}$)	Vis (km)	TP (°C)	RH (%)	WS (m/s)
Total	Aver.	193.9	378.7	13.1	224.1	58.7	13.4	4.8	-0.7	67.4	2.4
	SD	81.1	131.3	4.6	95.5	12.5	7.8	2.9	3.0	18.1	0.8
Haze	Aver.	255.0	474.1	16.5	305.8	60.1	8.8	2.8	-1.2	75.3	2.1
	SD	64.8	111.4	2.6	62.2	7.1	2.6	1.8	2.4	12.9	0.8
Non-haze	Aver.	136.6	289.2	9.8	147.4	41.9	17.8	6.7	-0.3	59.5	2.6
	SD	44.5	72.4	3.5	47.7	10.3	8.8	2.5	3.4	18.7	0.8
Non-haze/Haze		0.5	0.6	0.6	0.5	0.7	2.0	2.4	0.2	0.8	1.2

Vis: visibility, TP: temperature, RH: relative humidity, WS: wind speed.

days (173.9–361.0 $\mu\text{g m}^{-3}$ for PM_{2.5} and 344.0–745.5 $\mu\text{g m}^{-3}$ for TSP) than during non-haze days (62.5–218.1 $\mu\text{g m}^{-3}$ for PM_{2.5} and 165.7–416.1 $\mu\text{g m}^{-3}$ for TSP). The mean concentration of PM_{2.5}, TSP, BC, SO₂, and NO₂ increased by 78%, 63%, 69%, 92% and 50%, respectively, during haze days compared to those during non-haze days. The mean visibility during hazy days was 2.8 km, one third of that during non-haze days. In contrast, O₃ levels were much higher during non-haze days than during haze days, implying lower atmospheric oxidation potential during haze episodes. As expected, high RH and low wind speed were observed during haze days, which were conducive to air pollution accumulation (Cao et al., 2009; Ramachandran and Rajesh, 2007).

The average BC concentration was 16.5 $\mu\text{g m}^{-3}$ during haze episodes and 9.8 $\mu\text{g m}^{-3}$ during non-haze days. The frequency distribution of BC concentrations at the 5-min intervals is shown in Fig. 2. It can be seen that BC distribution is of significant difference between haze and non-haze periods. During haze days, BC frequency distribution exhibited an apparent “unimodal distribution” and peaked at 14–16 $\mu\text{g m}^{-3}$, which was mainly because stable meteorology conditions (RH = 75.3%; WS = 2.1 m s^{-1}) are conducive to BC accumulation. About 43% of the haze BC data are located in the range of 14–18 $\mu\text{g m}^{-3}$, and only ~2% of the data are below ~6 $\mu\text{g m}^{-3}$. This unimodal distribution during haze days was also found in a previous study of Cao et al. (2009). In contrast, non-haze BC distribution showed the “flat distribution” in the range of 2–18 $\mu\text{g m}^{-3}$, which was due to strong winds which facilitate fast dispersion and dilution. Only ~8% of the data were above 18.0 $\mu\text{g m}^{-3}$ during non-haze days.

Fig. 3 shows the diurnal variations of BC, SO₂, NO₂, and O₃ during

haze and non-haze days. BC concentrations during non-haze days showed a clear diurnal pattern with a bimodal distribution. The two peaks were located at around 08:00 a.m. and 20:00 PM, consistent with the traffic rush hours. In contrast, BC concentrations during haze days showed a rather stable diurnal pattern. The source emissions of BC were expected to be relative stable during the measurement period in the heating season. Therefore, high BC levels during haze episodes could be a consequence of stagnant weather conditions (WS = 2.1 m s^{-1}) which favored the accumulation of aerosol particles. The diurnal variations of two precursor gases, NO₂ and SO₂, showed inverse trends between haze and non-haze episodes, which could be explained by atmospheric diffusion and oxidation processes. The accumulation of pollutants under stagnant weather conditions likely caused the elevated SO₂ and NO₂ during haze days. Oxidation of SO₂ and NO₂ and subsequent gas-to-particle conversion also contributed to the diurnal variations of SO₂ and NO₂, which are further discussed in 3.4 below. The mean O₃ level during non-haze days was ~2.0 times of that during haze days. During non-haze days, the diurnal variations of O₃ exhibited a unimodal distribution with a high peak at about 15:00 PM. The mid-afternoon peak was mainly caused by strong O₃ formation under strong solar radiation and low NO₂ conditions (Wang et al., 2012; Shan et al., 2008). In contrast, the O₃ levels during haze episodes showed consistent low concentrations and smooth diurnal variations, which should be attributed to low solar radiations (low temperatures and visibilities) and high NO₂ levels (Wang et al., 2012). Apparently, atmospheric oxidation potential was relatively weaker during haze periods.

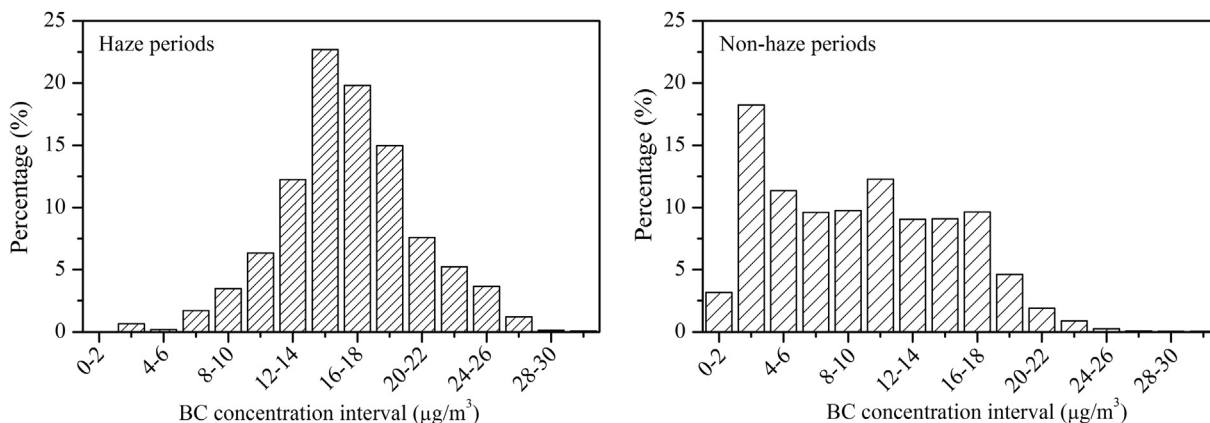


Fig. 2. Frequency distribution of 5-min BC data during haze and non-haze days.

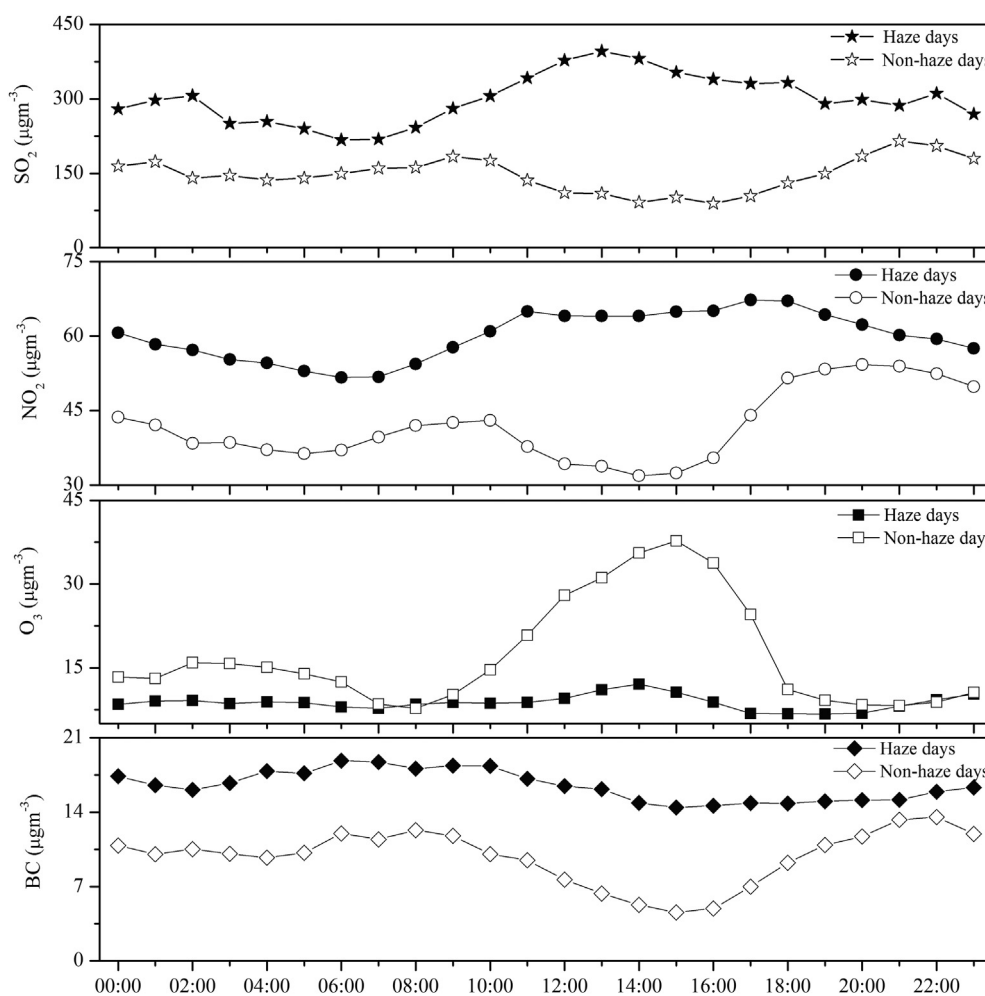


Fig. 3. Diurnal variation of the hourly averaged BC, SO₂, NO₂, and O₃ for both haze and non-haze days.

3.2. PM composition during haze and non-haze days

Table 2 shows the concentrations of water soluble ions in PM_{2.5} and TSP during haze and non-haze periods. The mean concentrations for the nine ions in TSP follow the same order of SO₄²⁻ > NO₃⁻ > NH₄⁺ > Ca²⁺ > Cl⁻ > K⁺ > Na⁺ > F⁻ > Mg²⁺ during both haze and non-haze days. However, a slightly different order

was found in PM_{2.5}, which showed SO₄²⁻ > NO₃⁻ > NH₄⁺ > Cl⁻ > K⁺ > Ca²⁺ > Na⁺ > F⁻ > Mg²⁺ (or Mg²⁺ > F⁻) during haze (or non-haze) days. The percentage contribution to PM_{2.5} from the total of the measured ions was 42.0% during haze episodes and 29.0% during non-haze episodes. Besides, the PM_{2.5}/TSP ratios for NO₃⁻, SO₄²⁻, NH₄⁺, Cl⁻, and K⁺ were all above 0.7, indicating that these chemical species were mainly present in fine particles in

Table 2
Concentrations for the Major Chemical Species in PM_{2.5} and TSP, and the Ratios of PM_{2.5}/TSP for haze and non-haze Events in Dec.2012 over Xi'an.

Concentration (μg/m ³)	Haze periods			Non-haze periods		
	TSP	PM _{2.5}	PM _{2.5} /TSP	TSP	PM _{2.5}	PM _{2.5} /TSP
Mass	474.1 ± 111.4	255.0 ± 64.8	0.5	289.2 ± 72.4	136.6 ± 44.5	0.5
Na ⁺	1.9 ± 0.5	1.3 ± 0.3	0.7	1.3 ± 0.4	0.8 ± 0.3	0.6
NH ₄ ⁺	23.6 ± 10.6	19.9 ± 8.7	0.8	7.7 ± 5.5	6.6 ± 4.5	0.9
K ⁺	4.5 ± 1.5	3.6 ± 1.2	0.8	1.8 ± 0.6	1.5 ± 0.5	0.8
Mg ²⁺	0.7 ± 0.1	0.3 ± 0.1	0.4	0.5 ± 0.1	0.2 ± 0.1	0.4
Ca ²⁺	10.8 ± 4.5	2.7 ± 2.0	0.3	8.6 ± 3.5	2.4 ± 1.3	0.3
F ⁻	1.5 ± 0.8	0.5 ± 0.3	0.3	0.6 ± 0.4	0.2 ± 0.2	0.3
Cl ⁻	11.6 ± 4.5	9.2 ± 3.8	0.8	5.2 ± 1.7	4.5 ± 1.5	0.9
NO ₃ ⁻	36.6 ± 16.0	28.5 ± 11.0	0.8	11.9 ± 8.9	9.8 ± 7.4	0.8
SO ₄ ²⁻	55.3 ± 30.2	40.4 ± 19.6	0.7	18.3 ± 11.6	13.5 ± 8.3	0.7
OC	67.3 ± 24.3	43.4 ± 12.9	0.6	41.5 ± 13.0	27.0 ± 6.0	0.7
EC	14.8 ± 3.6	9.5 ± 3.7	0.6	9.1 ± 3.1	6.9 ± 1.8	0.8
OC/EC	4.5	4.6	1.0	4.6	3.9	0.8

comparison with typical dust tracers, e.g. Ca²⁺ and Mg²⁺, that were mainly present in coarse particles. A high haze/non-haze ratio (2.9–3) was also found for NO₃⁻, SO₄²⁻, and NH₄⁺ in PM_{2.5} and TSP, indicating that more secondary inorganic aerosols were formed during haze period. As Xi'an is located in inland China, marine Cl⁻ origin should be negligible. The strong correlations ($r > 0.8$) were observed between biomass burning marker K⁺ (Shen et al., 2009) and Cl⁻, indicating Cl⁻ in this study is likely from biomass burning. It should be noted that the haze/non-haze ratios for Mg²⁺ and Ca²⁺ were about 1.3, implying that the contribution of crustal sources to PM varied slightly between haze and non-haze days.

The ion balance in PM_{2.5} and TSP during haze and non-haze episodes was calculated to evaluate the acidity of aerosol particles. The cation (C) and anion (A) micro-equivalent concentrations (m⁻³) were calculated as follows:

$$C = \text{Na}^+ / 23 + \text{NH}_4^+ / 18 + \text{K}^+ / 39 + \text{Mg}^{2+} / 12 + \text{Ca}^{2+} / 20$$

$$A = \text{F}^- / 19 + \text{Cl}^- / 35.5 + \text{NO}_3^- / 62 + \text{SO}_4^{2-} / 48$$

The ion balance results showed significant differences between haze and non-haze days for both PM_{2.5} and TSP (Fig. 4). For example, PM_{2.5} samples were close to neutral (from weak acidic to weak alkaline) during non-haze days, but were weakly to strong acidic during haze days. TSP samples were mostly alkaline during non-haze days and close to neutral during haze days. Strong acidity in PM_{2.5} samples during haze days could be attributed to the enrichment of sulfuric and nitric acid in fine particles, while the less acidity in TSP were due to the abundance of alkaline cations (e.g.,

Ca²⁺ and Mg²⁺) in coarse dust particles (see Table 2).

Table 2 shows that OC and EC in PM_{2.5} samples during haze days were about 1.6 and 1.4 times, respectively, of those during non-haze days. High PM_{2.5}/TSP ratios of OC and EC during both haze and non-haze days indicate that the carbonaceous species were enriched in fine particles. OC had higher concentrations than sulfate during both haze and non-haze episodes, implying that carbonaceous aerosols were important contributors to PM. OC consists of primary organic carbon (POC) and secondary organic carbon (SOC), with the former being emitted from sources directly while the latter being formed through gas-to-particle transformation (Turpin et al., 1991; Chow et al., 1996; Ho et al., 2002). Therefore, variations in OC/EC ratios between haze and non-haze episodes may reflect SOC production assuming that the emission sources were relatively stable during the measurement period. In this study, the average daily OC/EC ratio in PM_{2.5} was higher during haze days than during non-haze days (4.6 vs. 3.9), indicating more SOC production during haze episodes.

3.3. PM mass balance

The mass balance of TSP and PM_{2.5} during haze and non-haze days is shown in Fig. 5. Organic matter (OM) was calculated as OC multiplied by a factor of 1.6 (Viidanoja et al., 2001). In TSP samples, the contributions from the three major secondary inorganic aerosol species (NH₄⁺, SO₄²⁻, and NO₃⁻) were higher during haze days than during non-haze days (24% vs 13%), and correspondingly, dust and other undetected materials, which were the largest contributors to TSP, accounted less fractions during haze days (47% vs 59%). A

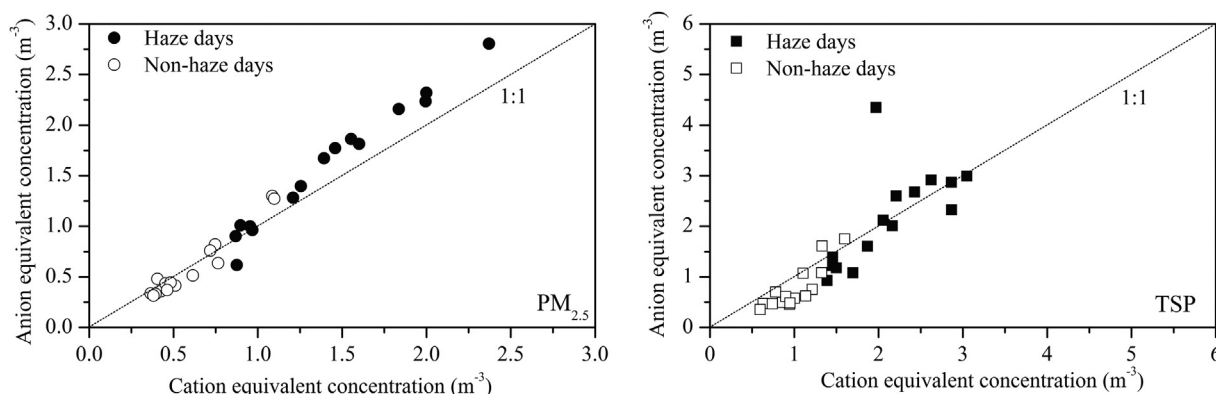


Fig. 4. Ion balance of cationic (Na⁺, NH₄⁺, K⁺, Mg²⁺, and Ca²⁺) and anionic (F⁻, Cl⁻, NO₃⁻ and SO₄²⁻) species in PM_{2.5} and TSP for haze and non-haze days.

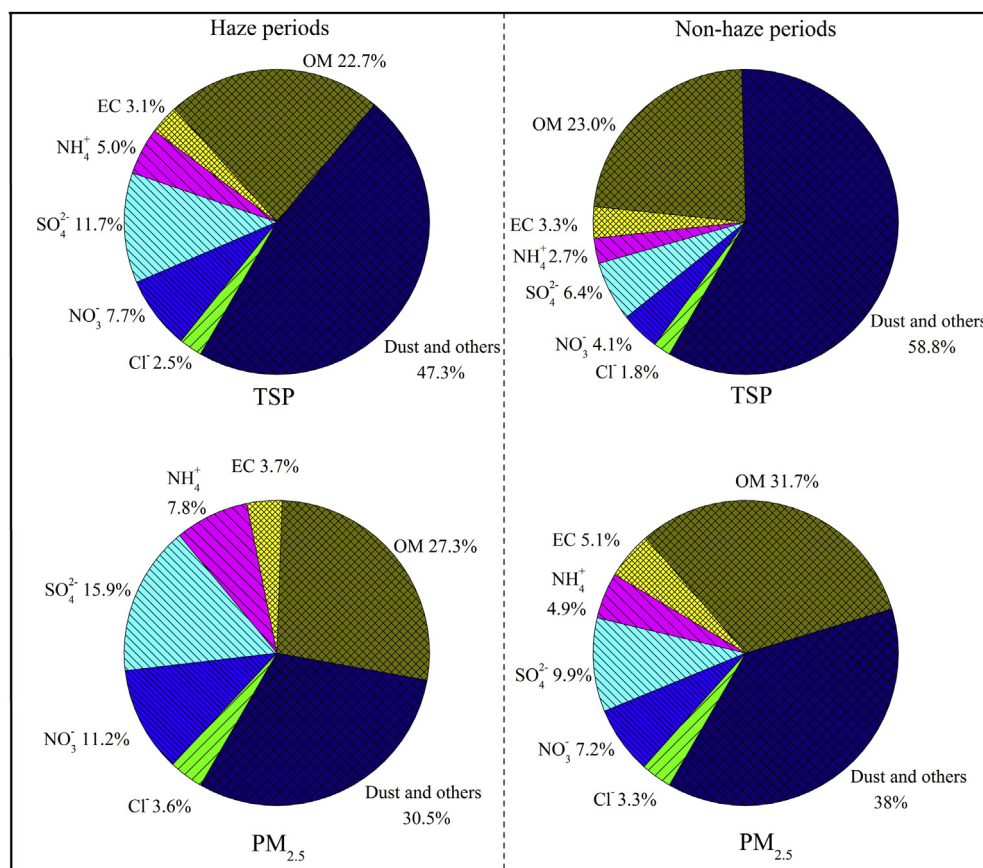


Fig. 5. Fractional contributions of the major chemical species to the TSP and PM_{2.5} mass at Xi'an for haze and non-haze days.

similar trend was also found for PM_{2.5} samples. Thus, secondary aerosol formation was identified as a key factor for haze formation. Interestingly, dust and undetected materials constituted the largest fraction (around 30–40%) in PM_{2.5} during both haze and non-haze periods in Xi'an, a phenomenon that is consistent with findings in several recent studies (Shen et al., 2010; Cao et al., 2012; Huang et al., 2014). This phenomenon was caused by high dust loading in this region because of its location in the south margin of Chinese Loess Plateau and limited precipitation amount in this area (Shen et al., 2012). Results presented here suggest that controlling fugitive dust could be an effective strategy in mitigating particle pollution in arid and semi-arid cities like Xi'an.

3.4. Transformation mechanism of PM during haze days

As mentioned above, EC is directly emitted from combustion processes and can be taken as a tracer of primary anthropogenic emissions. Sulfate, nitrate, and ammonium are secondary inorganic aerosols (SIA), which are formed from the gas (such as SO₂, NO₂, and NH₃) - particle transformation through chemical reactions (Seinfeld, 1986; Li-Jones and Prospero, 1998). Thus, differences between haze and non-haze events in the ratios of PM_{2.5} chemical species to EC can provide some insights on the transformation mechanisms.

Fig. 6 shows mass concentrations of eleven species and their ratios to EC concentration during haze and non-haze days. The ratios of SO₄²⁻/EC, NO₃⁻/EC, and NH₄⁺/EC during haze days are about two times of those during non-haze days, indicating elevated formation of secondary inorganic aerosols during haze days. There are normally three chemical pathways that lead to the formation of

SO₄²⁻ and NO₃⁻, including gas-phase reactions of SO₂ and NO₂ with OH radical and O₃, aqueous transformation (metal-catalyzed oxidation or H₂O₂/O₃ oxidation), and in-cloud processes. Gas-phase oxidation of SO₂ to SO₄²⁻ by OH radical is strongly temperature dependent (Seinfeld, 1986). In this study, low temperatures and weak atmospheric oxidizing capacities were observed during haze episodes, implying limited sulfate and nitrate formation through radical oxidation process. In contrast, high RH (75.3% on average) during haze days should favor aqueous transformation for sulfate and nitrate formation. Previous studies discussed in detail the formation mechanisms of SO₄²⁻ and NO₃⁻ from their precursors. These include heterogeneous reactions in aqueous surface layer of pre-existing particles or dissolve into water under catalyze oxidation (metal or H₂O₂/O₃), homogeneous gas phase reaction of SO₂ and NO_x with OH radical, and direct photochemical reactions of SO₄²⁻ and NO₃⁻ (Yao et al., 2003; Ding et al., 2003; Wang et al., 2002; Seinfeld, 1986). Generally, heterogeneous conversion efficiency is strongly influenced by RH, especially during pollution episodes. In contrast, homogeneous gas phase reactions and photochemical reactions depend on temperature. As photochemical reactions were very limited under low temperatures and atmospheric oxidation capacities during haze episodes, heterogeneous reactions through metal-catalyzed oxidation should be the main mechanism for the observed high efficiency of sulfate and nitrate formation.

However, OC/EC ratio during haze days was 4.6, only slightly higher than the value of 3.9 during non-haze days. The difference in OC/EC between haze and non-haze days was not as significant as that for SIA/EC. This suggests that the increase in SOC was not as much as that in SIA during haze days. To investigate the SOC contribution to OC, the EC-tracer method proposed by Turpin and

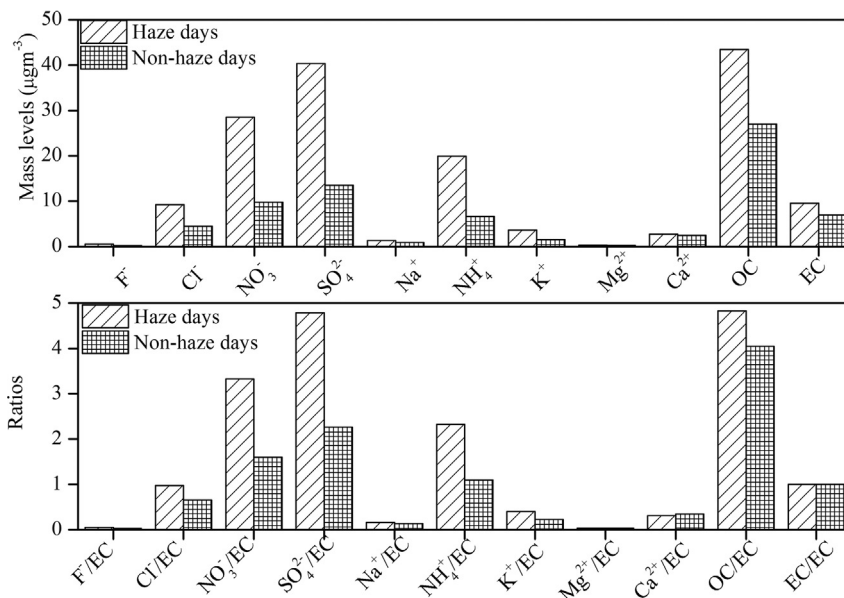


Fig. 6. The mass concentrations of major species and their ratios with EC for PM_{2.5} in haze and non-haze days.

Huntzicker (1995) was used to estimate SOC concentration:

$$\text{SOC} = \text{OC}_{\text{tot}} - \text{EC} * (\text{OC}/\text{EC})_{\text{min}}$$

where OC_{tot} is the total of OC (TOC), and $(\text{OC}/\text{EC})_{\text{min}}$ is the minimum OC/EC ratio observed during the study periods. The estimated SOC ranged between 4.4 and 31.9 $\mu\text{g m}^{-3}$ with an average of 14.7 $\mu\text{g m}^{-3}$ during haze days, which gave a percentage contribution of 9.6%–57.5% with a mean value of 33.4% to OC in PM_{2.5}. In contrast, the estimated SOC was much lower during non-haze days, varying between 0.9 and 18.3 $\mu\text{g m}^{-3}$ with an average of 6.0 $\mu\text{g m}^{-3}$, which gave a percentage contribution of 3.2%–58.1% with a mean value of 21.3%.

It should be noted that SOC is mainly formed from the oxidation of volatile or semi-volatile organic compounds and is prevalent in summer because of high photochemical oxidation potentials. Winter SOC is frequently ignored presumably because SOC level is assumed to be low considering the low photochemical activities in winter. However, this might not always be the case, especially during haze days when stagnant air, high RH, and low temperature favored the partitioning of SVOCs to the particle phase through aqueous reactions (Strader et al., 1999; Shrivastava et al., 2008; Chen et al., 2010). For example, model predicted winter average SOA concentration across the entire San Joaquin Valley in California accounted for approximately 20% of the total organic aerosols using the UCD/CIT air quality model with the Caltech Atmospheric Chemistry Mechanism (Chen et al., 2010). In addition, acidic aerosols also promote the formation of SOC. For example, free acidity in atmosphere is necessary for the heterogeneous polymerization of isoprene (Ferek et al., 1983; Staebler et al., 1999; Limbeck et al., 2003). High RH and stronger PM_{2.5} acidity during haze episodes should also favor the SOC formation. Results presented in this study showed significant wintertime SOC formation during haze days, consistent with findings of recent study in China (Huang et al., 2014). The formation pathways of SOC may include OH radical initiated oxidation, NO₃ radical initiated nocturnal chemistry, and aqueous-phase chemistry. The SOC formation may be enhanced by increased gas-to-particle partitioning at low temperatures. Furthermore, high RH and stagnant weather condition may also promote the SOC formation.

4. Conclusions

PM, BC, SO₂, and NO₂ concentrations in Xi'an were much higher during haze days than during non-haze days, while O₃ exhibited an opposite pattern. Different patterns were observed between haze and non-haze days in BC frequency distributions and diurnal variations, indicating the accumulation of BC during haze episodes. The sum of the three major secondary inorganic species (SO₄²⁻, NO₃⁻, and NH₄⁺) during haze days was about 3 times of that during non-haze days, leading to acidic PM_{2.5} during haze days. The ratios of SO₄²⁻/EC, NO₃⁻/EC, and NH₄⁺/EC were significantly enhanced from non-haze to haze days, suggesting that aqueous transformation under high RH condition played an important role on secondary inorganic species formation. In contrast, OC/EC ratios from non-haze to haze days varied less than those of the secondary inorganic species, showing the different formation mechanisms of SIA and SOC. SOC accounted nearly one third of OC on average during haze days, highlighting the significance of SOC formation in wintertime haze events.

Acknowledgements

This research is financially supported by the Fundamental Research Funds for Central Universities of China (xkjc2015002), the Key Lab of Aerosol Chemistry & Physics, Chinese Academy of Sciences (KLAC200501), and the Ministry of Science and Technology of China (2013FY112700).

References

- Cao, J.J., Lee, S.C., Ho, K.F., Zhang, X.Y., Zou, S.C., Fung, K., Chow, J.C., Watson, J.G., 2003. Characteristics of carbonaceous aerosol in Pearl River Delta Region, China during 2001 winter period. *Atmos. Environ.* 37, 1451–1460.
- Cao, J.J., Zhu, C.S., Chow, J.C., Watson, J.G., Lee, S.C., Han, Y.M., Wang, G.H., Shen, Z.X., An, Z.S., 2009. Black carbon relationships with emissions and meteorology in Xi'an, China. *Atmos. Res.* 94, 194–202.
- Cao, J.J., Shen, Z.X., Chow, J.C., Watson, J.G., Lee, S.C., Tie, X.X., Ho, K.F., Wang, G.H., Han, Y.M., 2012. Winter and summer PM_{2.5} chemical compositions in fourteen Chinese cities. *J. Air Waste Manag. Assoc.* 62, 1214–1226.
- Chang, L.T.C., Tsai, J.H., Lin, J.M., Huang, Y.S., Chiang, H.L., 2011. Particulate matter and gaseous pollutants during a tropical storm and air pollution episode in southern Taiwan. *Atmos. Res.* 99, 67–79.
- Chen, J.J., Ying, Q., Kleeman, M.J., 2010. Source apportionment of wintertime

- secondary organic aerosol during the California regional PM₁₀/PM_{2.5} air quality study. *Atmos. Environ.* 44, 1331–1340.
- Chen, L.W.A., Chow, J.C., Doddridge, B.G., Dickerson, R.R., Ryan, W.F., Mueller, P.K., 2003. Analysis of a summertime PM_{2.5} and haze episode in the mid-Atlantic region. *J. Air Waste Manag. Assoc.* 53, 946–956.
- Cheng, C.L., Wang, G.H., Zhou, B.H., Meng, J.J., Li, J.J., Cao, J.J., Xiao, S., 2013. Comparison of dicarboxylic acids and related compounds in aerosol samples collected in Xi'an, China during haze and clean periods. *Atmos. Environ.* 81, 443–449.
- Chow, J.C., Watson, J.G., Lu, Z., Lowenthal, D.H., Frazier, C.A., Solomon, P.A., Thuillier, R.H., Magliano, K., 1996. Descriptive analysis of PM_{2.5} and PM₁₀ at regionally representative locations during SIVAQS/AUSPEX. *Atmos. Environ.* 30, 2079–2112.
- Chow, J.C., Watson, J.G., Chen, L.W.A., Arnott, W.P., Moosmuller, H., 2004. Equivalence of elemental carbon by thermal/optical reflectance and transmittance with different temperature protocols. *Environ. Sci. Technol.* 8, 4414–4422.
- Du, H.H., Kong, L.D., Cheng, T.T., Chen, J.M., Du, J.F., Li, L., Xia, G.X., Leng, C.P., Huang, G.H., 2011. Insights into summertime haze pollution events over Shanghai based on online water-soluble ionic composition of aerosols. *Atmos. Environ.* 45, 5131–5137.
- Ding, J., Zhu, T., 2003. Heterogeneous reactions on the surface of fine particles in the atmosphere. *China Sci. Bull.* 48, 2267–2276.
- Ferek, R., Lazrus, A., Haagenson, P., Winchester, J.W., 1983. Strong and weak acidity of aerosols collected over the north-eastern United States. *Environ. Sci. Technol.* 17, 315–324.
- Ho, K.F., Lee, S.C., Yu, J.C., Zou, S.C., Fung, K., 2002. Carbonaceous characteristics of atmospheric particulate matter in Hong Kong. *Sci. Total Environ.* 300, 59–67.
- Huang, R.J., Zhang, Y.L., Bozzetti, C., Ho, K.F., Cao, J.J., Han, Y.M., Daellenbach, K.R., Slowik, J.G., Platt, S.M., Canonaco, F., Zotter, P., Wolf, R., Pieber, S.M., Bruns, E.A., Crippa, M., Ciarelli, G., Piazzalunga, A., Schwikowski, M., Abbaszade, G., Schnelle-Kreis, J., Zimmermann, R., An, Z.S., Szidat, S., Baltensperger, U., Haddad, I.E., Prevot, A.S., 2014. High secondary aerosol contribution to particulate pollution during haze events in China. *Nature* 514, 218–222.
- Jung, J.S., Lee, H.L., Kim, Y.J., Liu, X.G., Zhang, Y.H., Gu, J.W., Fan, S.J., 2009. Aerosol chemistry and the effect of aerosol water content on visibility impairment and radiative forcing in Guangzhou during the 2006 Pearl River Delta campaign. *J. Environ. Manag.* 90, 3231–3244.
- Kang, C.M., Lee, H.S., Kang, B.W., Lee, S.K., Sunwoo, Y., 2004. Chemical characteristics of acidic gas pollutants and PM_{2.5} species during hazy episodes in Seoul, South Korea. *Atmos. Environ.* 38, 4749–4760.
- Li-Jones, X., Prospero, J.M., 1998. Variations in the size distribution of non-sea-salt sulfate aerosol in the marine boundary layer at Barbados: impact of African dust. *J. Geophys. Res.* 103, 16073–16084.
- Limbeck, A., Kulmala, M., Puxbaum, H., 2003. Secondary organic aerosol formation in the atmosphere via heterogeneous reaction of gaseous isoprene on acidic particles. *Geophys. Res. Lett.* 30, 19.
- Oanh, N.T.K., Leelasakultum, K., 2011. Analysis of meteorology and emission in haze episode prevalence over mountain-bounded region for early warning. *Sci. Total Environ.* 409, 2261–2271.
- Odmana, M.T., Hu, Y.T., Russell, A.G., Hanedar, A., Boylan, J.W., Brewer, P.F., 2009. Quantifying the sources of ozone, fine particulate matter, and regional haze in the Southeastern United States. *J. Environ. Manag.* 90, 3155–3168.
- Petzold, A., Kramer, H., Schonlinner, M., 2002. Continuous measurement of atmospheric black carbon using a multi-angle absorption photometer. *Environ. Sci. Pollut. Res.* 4, 78–82.
- Ramachandran, S., Rajesh, T.A., 2007. Black carbon aerosol mass concentrations over Ahmedabad, an urban location in western India: comparison with urban sites in Asia, Europe, Canada, and the United States. *J. Geophys. Res.* 112, D06211.
- Schichtel, B.A., Husar, R.B., Falke, S.R., Wilson, W.E., 2001. Haze trends over the United States, 1980–1995. *Atmos. Environ.* 35, 5205–5210.
- Seinfeld, J.H., 1986. *Atmospheric Chemistry and Physics of Air Pollution*. Wiley, New York.
- Shan, W., Yin, Y., Zhang, J., Ding, Y.P., 2008. Observational study of surface ozone at an urban site in East China. *Atmos. Res.* 89, 252–261.
- Shen, Z.X., Cao, J.J., Arimoto, R., Zhang, R.J., Jie, D.M., Liu, S.X., Zhu, C.S., 2007. Chemical composition and source characterization of spring aerosol over Horqin sand land in northeastern China. *J. Geophys. Res.* 112, D14315.
- Shen, Z.X., Arimoto, R., Cao, J.J., Zhang, R.J., Li, X.X., Du, N., Okuda, T., Nakao, S., Tanaka, S., 2008. Seasonal variations and evidence for the effectiveness of pollution controls on water-soluble inorganic species in total suspended particulates and fine particulate matter from Xi'an, China. *J. Air Waste Manag. Assoc.* 58, 1560–1570.
- Shen, Z.X., Cao, J.J., Arimoto, R., Han, Z.W., Zhang, R.J., Han, Y.M., Liu, S.X., Okuda, T., Nakao, S., Tanaka, S., 2009. Ionic composition of TSP and PM_{2.5} during dust storms and air pollution. *Atmos. Environ.* 43, 2911–2918.
- Shen, Z.X., Cao, J.J., Arimoto, R., Han, Y.M., Zhu, C.S., Tian, J., Liu, S.X., 2010. Chemical characteristics of Fine particles (PM₁) from Xi'an, China. *Aerosol Sci. Tech.* 44 (6), 461–472.
- Shen, Z.X., Cao, J.J., Liu, S.X., Zhu, C.S., Wang, X., Zhang, T., Xu, H.M., Hu, T.F., 2011. Chemical composition of PM₁₀ and PM_{2.5} collected at ground level and 100 meters during a strong winter-time pollution episode in Xi'an, China. *J. Air Waste Manag. Assoc.* 61, 1150–1159.
- Shen, Z.X., Zhang, L.M., Cao, J.J., Tian, J., Liu, L., Wang, G.H., Zhao, Z.Z., Wang, X., Zhang, R.J., Liu, S.X., 2012. Chemical composition, sources, and deposition fluxes of water-soluble inorganic ions obtained from precipitation chemistry measurements collected at an urban site in northwest China. *J. Environ. Monit.* 14, 3000–3008.
- Shen, Z.X., Cao, J.J., Zhang, L.M., Liu, L., Zhang, Q., Li, J.J., Han, Y.M., Zhu, C.S., Zhao, Z.Z., Liu, S.X., 2014. Day–night differences and seasonal variations of chemical species in PM₁₀ over Xi'an, northwest China. *Environ. Sci. Pollut. Res.* 21, 3697–3705.
- Sheridan, P.J., Arnott, W.P., Ogren, J.A., Andrews, E., Arkinson, D.B., Covert, D.S., Moosmüller, H., Petzold, A., Schmid, B., Strawah, A.W., Varmab, R., Virkkula, A., 2005. The Reno aerosol optics study: an evaluation of aerosol absorption measurement methods. *Aerosol Sci. Technol.* 39, 1–16.
- Shrivastava, M.K., Lane, T.E., Donahue, N.M., Pandis, S.N., Robinson, A.L., 2008. Effects of gas particle partitioning and aging of primary emissions on urban and regional organic aerosol concentrations. *J. Geophys. Res.* 113, D18301.
- Staebler, R., Toom-Sauntry, D., Barrie, L., Langendorfer, U., Lehrer, E., Li, S.M., Clark, H.D., 1999. Physical and chemical characteristics of aerosols at Spitsbergen in the spring of 1996. *J. Geophys. Res.* 104, 5515–5529.
- Strader, R., Lurmann, F., Pandis, S.N., 1999. Evaluation of secondary organic aerosol formation in winter. *Atmos. Environ.* 33, 4849–4863.
- Tao, J., Zhang, L.M., Gao, J.J., Wang, H., Chai, F.H., Wang, S.L., 2015. Aerosol chemical composition and light scattering during a winter season in Beijing. *Atmos. Environ.* 110, 36–44.
- Turpin, B.J., Huntzicker, J.J., Larson, S.M., Cass, G.R., 1991. Los Angeles mid-day particulate carbon: primary and secondary aerosol. *Environ. Sci. Technol.* 25, 1788–1793.
- Turpin, B.J., Huntzicker, J.J., 1995. Identification of secondary organic aerosol episodes and quantitation of primary and secondary organic aerosol concentrations during SCAQS. *Atmos. Environ.* 29, 3527–3544.
- Viidanoja, J., Sillanpaa, M., Laakia, J., Kerminrn, V.M., Hillamo, R., Aarnio, P., Koskentalo, T., 2001. Organic and black carbon in PM_{2.5} and PM₁₀: 1 year of data from an urban site in Helsinki, Finland. *Atmos. Environ.* 36, 3183–3193.
- Wang, G., Huang, L., Gao, S., Gao, S.T., Wang, L.S., 2002. Characterization of water-soluble species of PM₁₀ and PM_{2.5} aerosols in urban area in Nanjing, China. *Atmos. Environ.* 36, 1299–1307.
- Wang, X., Shen, Z.X., Cao, J.J., Zhang, L.M., Liu, L., Li, J.J., Liu, S.X., Sun, Y.F., 2012. Characteristics of surface ozone at an urban site of Xi'an in Northwest China. *J. Environ. Monit.* 14, 116.
- Wang, Y., Zhuang, G., Sun, Y., An, Z.S., 2006. The variation of characteristics and formation mechanisms of aerosols in dust, haze, and clear days in Beijing. *Atmos. Environ.* 40, 6579–6591.
- Yadav, A.K., Kumar, K., Kasim, A.M.B.H., Parida, S.K., Sharan, M., 2003. Visibility and incidence of respiratory diseases during the 1998 haze episode in Brunei Darussalam. *Pure Appl. Geophys.* 13, 265–277.
- Yan, Q., Hua, D.X., Wang, Y.F., Li, S.C., Gao, F., Zhou, Z.R., Wang, L., Liu, C.X., Zhang, S.Q., 2013. Observations of the boundary layer structure and aerosol properties over Xi'an using an eye-safe Mie scattering Lidar. *J. Quant. Spectrosc. Radiat. Transf.* 112, 97–105.
- Yao, X.H., Lau, A.P.S., Fang, M., Chan, C.K., Hu, M., 2003. Size distributions and formation of ionic species in atmospheric particulate pollutants in Beijing, China: 1-inorganic ions. *Atmos. Environ.* 37, 2991–3000.